

Resistance of through-plate component in beam-to-column joints with circular hollow columns

Hoang Van-Long, Demonceau Jean-François, and Jaspart Jean-Pierre
ArGEnCo Department, University of Liège, Belgium

Abstract

A configuration of beam-to-column joint with circular hollow section columns is proposed. A vertical plate, called through-plate, passing through the column is used to support the beams. In order to facilitate connecting the beams, two horizontal plates, each side of the column, are welded to the upper side of the through-plate. The lower flanges of the steel beams are connected to the horizontal plates by bolts, and the upper flanges are attached to the concrete slab by shear connections. The joint is considered as hinges in the construction phase while semi-rigid and partial strength can be adopted for the joint behaviour during the exploitation time. A development on the through-plate component of the joint is presented in this paper. Global behaviour of the joint under hogging moment and shear force is analysed leading to a mechanical model of the through-plate component. Using the elastic buckling theory of plates, the analytical formulas for critical stresses of the through-plate are obtained. The coefficients taking into account boundary conditions, material plasticity and geometrical imperfection are determined by finite element analysis. The proposed model is validated by experimental results showing a good accuracy. The design guideline for the component is finally provided for the practical purpose.

Key words: beam-to-column joints; finite element analysis; experimental tests; component method

1. Introduction

Within a European project entitled “ATTEL: Performance-based approaches for high-strength tubular columns and connections under earthquake and fire loadings” and funded by RFCS (Research Fund for Coal and Steel), one of the objectives is to provide building types where the use of high strength steel tubes for the columns can give the economic benefit [1]. In the case of static loading, a type of building has been proposed, from the global structural solution to the detail on the connections including the design guidelines.

Concerning the global structural solution, a schematic view on the economic advantage of using high strength steel (up to S700) in comparison with normal steel (S355) has been pointed out [2]. From the conclusions of the research, one type of frames with the following characteristics is recommended to use high strength steel for the columns: a large number of spans, the spans are large, and the number of storeys is small. In the practice of constructions, it can see this building type in commercial centres, parkings, airports, etc. In these frames, it can observe that the axial forces in the columns are preponderant in comparison with bending moment, and the bending moments in the connections almost come from vertical loads.

With respect to base joints, simple column bases using rectangular end- plate with four anchor bolts has been suggested, and the design guideline has been provide [3].

As far as the beam-to-column joints are concerned, the configuration shown on Fig.1 is proposed. In the joint, one through-plate is welded to the column, on this plate two horizontal plates (each side of the column) are attached by fillet welds. The lower flanges of the steel beams are connected to the horizontal plates by bolts while the upper flanges are attached to the concrete slab by shear connections. The outside part of the through-plate may be rectangular or triangular shapes. This joint can be considered as an economic solution, because a modest volume of material is consumed, also the fabrication and construction procedures are quite simple leading to the reduction of build-up time. On the structural behaviour aspect, the joints is considered as hinges in the construction phrase while during the exploitation time the joint maybe becomes a semi-rigid and partial strength connection due to the collaboration of the reinforced concrete slab. As in most practical cases, profiled steel sheets are recommended to use in the composite slab, so that during the concrete casting time the lateral stability of the steel beams can be assumed by these steel sheets.

Concerning the design rule for the beam-to-column joint, by using the component method concept, the joints can be decomposed into the following components:

- longitudinal slab reinforcement in tension;
- bolts in shear (bolt shank in shear and associated plates in bearing);
- welds in shear (through-plate to column and horizontal plates to through-plate welds);

- through-plate and column in diagonal compression (combine of vertical and horizontal loads).

The detail calculation for the characterizations of the “longitudinal slab reinforcement in tension” component can found the literature, e.g [4], while the “bolts in shear”, “plate in bearing” and “weld in shear” components are covered by Eurocode-3, part 1-8 [5]. This paper presents a development on the “through-plate and column in diagonal compression” component that is not available in the current codes and literatures. The failure mode of the through-plate component is identified and then the mechanical models for the component is proposed (Section 2). The proposed models is analytically formulated by using the linear elastic buckling theory of plates; and the correction coefficients taking into account the nonlinear parameters are determined through numerical studies (Section 3). Validation of the proposed model and formulas by experimental results are presented in Section 4. The practical design guideline for the component, including calculation examples, is drawn and presented in Section 5. Section 6 concerns the concluding remarks.

2. Assumptions and modelling

Let us examine the joint behaviour under a hogging moment and a shear force, as the situation during the exploitation time. In order to highlight the behaviour of the through-plate, it supposes that the failure does not occur in the bolts and the welds. As the friction between the concrete slab and the column can be negligible, the vertical load at the connection is therefore completely transferred from the steel beam web to the through-plate. On the other hand, the bending moment is equilibrium by two opposite horizontal forces, in tension on the top and in compression on the bottom; the tension force is supported by the reinforcement rebars in the concrete slab while the compression force is transferred to the through-plate. By consequence, a system comprising the beam web, the lower beam flanges and the through-plate has a risk of buckling under the diagonal compression (Fig.2). The reinforcement concrete slab and the steel column may be considered as the boundaries assuming the stability of the mentioned system. The relative rotation between the lower flanges of the beams and the horizontal plates may be negligible because they are attached one to other by the bolts. It can be imagined that the beam ends and the outside part of the through-plate are warped while the inside part of the through-plate is laterally buckled (Figs. 2 and 3). The studies on the buckling of the whole system are quite

complicated, for the sake of simplification, the following assumptions are made in order to separately study on each part.

- (1) The column wall including the welds can fix the rotation (around the column axis) and the vertical displacement of the through-plate; on the contrary, the reaction of the column wall to the longitudinal displacement (in the beam axis direction) of the through-plate is supposed to be small and negligible. With this assumption, the outside and inside parts can be separately modelled, and the effects of the column are modelled by the ideal boundary conditions: full clamp for the rotation and the vertical displacement or free for the longitudinal displacement.
- (2) The calculation of the loads transferred from the outside part to the inside part is based on the hypotheses that the outside part is considered as a cantilever beam.
- (3) The outside parts of the through-plate and the steel beam ends are also considered separately, only their interaction forces in the plan of the through-plate (or beam web) are examined, the torsional interaction is neglected. This assumption may be a bit conservative in the exploitation phase but in the construction phase where the composite slab is in execution this assumption should be considered. The considered interaction force is decomposed in two components, the horizontal component is supposed to be uniform distribution while a triangular distribution is assumed for the vertical component (Fig.4).
- (4) The deformation of the upper edge of the outside part of the through-plate, along the weld between the through-plate and the horizontal plate, is locked. This assumption aims to take into account the effects of the horizontal plate and the welds on the out of plan deformation of the outside part. Noting that there is a gap between the horizontal plate and the column, in this zone the deformation of the upper edge of the through-plate is permitted.

It would to note that among above assumptions, the assumptions (1) and (2), almost concerning the behaviour of the inside part, should be verified by experimental tests. On the other hand, the construction phase situation is used in the assumption (3) meaning that this assumption is quite conservative. As the assumption (4) is quite clear and it can be theoretically accepted.

Using the mentioned assumptions, the through-plate can be modelled by two separate parts, the inside part and the outside part, at their common bound the displacement are compatibility and the forces are equilibrium. The inside part is considered as a rectangular plate clamped in two vertical edges and two other edges are free, under compression stress on the clamped bounds (Fig.4). The outside part with rectangular or triangular shape, one vertical side is clamped and others are free; subjected to a uniform horizontal force combining with a triangular vertical force, on the upper edge. The loads, represented by force per length unit, acting on the outside part and the inside part may be determined through the following equations:

$$p = \frac{2V_{Ed}}{b-c} \quad (1)$$

$$f = \frac{F_{Ed}}{b-c} = \frac{V_{Ed}}{\tan \alpha (b-c)} = \frac{p}{2 \tan \alpha} \quad (2)$$

$$q_s = \frac{4F_{Ed}}{h} - \frac{V_{Ed}(4b+2c)}{h^2} \quad (3)$$

$$q_i = \frac{V_{Ed}(4b+2c)}{h^2} - \frac{2F_{Ed}}{h} \quad (4)$$

The following notations are used for geometrical, material and loading parameters of the through-plate (Figs. 4 and 5):

b is the width of the outside part;

c is the gap between the horizontal plate and the column face;

D is the outside diameter of the column;

E is Young modulus of the through-plate material;

F_{Ed} is the design value of the horizontal component of the load;

f_y is the yield strength of steel used for the through-plate ;

h is the height of the through-plate;

t is the thickness of the through-plate;

V_{Ed} is the design value of the vertical component of the load;

α is the load direction;

ν is Poisson ratio of the through-plate material.

3. Buckling loads for the outside and inside parts of the through-plate

3.1. Formulation

Using the buckling theory of plates, the critical stresses of the inside and outside parts can be written by Eqs.(5) and (6) as follows:

$$\sigma_{c, ou} = \mu_1 \frac{\pi^2 E}{12(1-\nu^2)} \left(\frac{t}{b} \right)^2; \quad (5)$$

$$\sigma_{c, in} = \mu_2 \frac{\pi^2 E}{12(1-\nu^2)} \left(\frac{t}{h} \right)^2. \quad (6)$$

The μ_1 and μ_2 coefficients in Eqs. (5) and (6) are used to take into account boundary conditions, loading conditions, plasticity of material, geometric imperfections and also the shear deformation of thick plates. The determination of these coefficients by the analytical way for the present cases is quite complicated so they are estimated by the numerical analysis in this work, as Eqs.(7) and (8):

$$\mu_1 = (\sigma_{c, ou})_{numerical} / \left(\frac{\pi^2 E}{12(1-\nu^2)} \left(\frac{t}{b} \right)^2 \right); \quad (7)$$

$$\mu_2 = (\sigma_{c, in})_{numerical} / \left(\frac{\pi^2 E}{12(1-\nu^2)} \left(\frac{t}{h} \right)^2 \right). \quad (8)$$

with $\sigma_{numerical}$ is calculated by numerical calculations using finite element (FE) method.

3.2. Determination of μ_1 and μ_2 coefficients

3.2.1. FE model of plates

LAGAMINE software is used for the numerical investigation, it is a nonlinear finite element computer program developed at Liege University [6]. The plates are modelled by 3D solid elements in which the large deformation and the plastic nonlinear material can be introduced.

Before modelling for the present cases, the numerical model is assessed by the analytical results on some classic examples existing in the literature. It is well known that the plasticity of material has been taken into account for the buckling analysis of plates in Bleich work [7] of which the results are recognized. Recently, Wang et al [8] have developed the buckling load for elastic/plastic rectangular or circular thick plates with the specific boundary conditions by using the incremental theory (IT) and deformation theory (DT) of the plasticity. The numerical results in the present paper will be compared with the results given by the mentioned works [7, 8] through two following examples.

Example 1: considering a square plate with simple supports on four its sides, under uniaxial load (Fig.6). Elastic modulus $E=10700$ ksi, yield strength $\sigma_0=61.4$ ksi. Ramberg-Osgood material, $\varepsilon = \sigma / E + k\sigma_0 / E(\sigma_0 / E)^c$, with $c=20$ and $k=0.3485$ is applied in [8] while the material described in Fig.7 is introduced in LAGAMINE. The initial imperfection $1/200$ as the recommendation in Eurocode 3, part 1-5 [9] is adopted in the numerical analysis (Fig.6b). Due to the symmetric of the material, the geometry and also the loadings, only $1/4$ part of the plate is modelled (Fig.6c). The comparison of the results is presented in Table 1 from which it can observe that the numerical results are in agreement with the Bleich's results and also with DT.

Example 2: a quite thick plate is considered in this example with thickness/width ratio equals to 0.075; two opposite edges are simply supported and others are free on which the uniform stresses apply (Fig.8). The material model and the initial imperfection used in the example 1 are again adopted in the present example. Young modulus/yield strength ratio (Ramberg-Osgood parameter) for the material is varied. The comparison of the results is reported in Table 2 pointing out that the numerical results are in agreement with DT results. It can say that in this case the buckling stress factors coming from IT in [8] are not reasonable because they don't change when yield strength varies.

From the examples, it can say that the above numerical model, as meshing, element type, material modelling, initial imperfection modelling, and boundary condition modelling can be used to determine the buckling loads of plates.

3.2.2. Determination of μ_1 and μ_2 coefficients

The mechanical models for the outside and inside parts of the through plate (Fig.4) are introduced in the FE on which the meshing, the element type, and the material modelling are already presented in Section 3.2.1. With respect to the geometric imperfection modelling, the value of 1/200 of the span is again used with the forms shown on Fig.9. As S355 steel is the most popular steel grade in markets, this steel characteristics are introduced in the FE models. In order to cover almost practical possibilities, the following parameters are varied (see Fig.5 for the notices):

- the load direction for the outside part, α vary from 15^0 to 90^0 ;
- the thickness/width ratio of the outside part, t/b vary from 0.05 to 0.15;
- the height/width ratio of the outside part, h/b vary from 0.6 to 1.4;
- three distribution types the load type for the inside part: bi-triangular, triangular and uniform (Fig.10);
- the thickness/high ratio of the inside part, t/h vary from 0.05 to 0.15;
- the width/high ratio of the inside part, D/h vary from 0.6 to 1.4;
- the value c of the gap between the horizontal plate and the column (Fig.4) equals to $0.1b$.

The FE analysis is used to compute the buckling stress, $\sigma_{\text{numerical}}$, then the μ_1 and μ_2 coefficients are calculated from Eqs.(7) and (8), the detail values are presented in Tables 3 and 4. The curves describing the tendencies of the μ_1 and μ_2 coefficients are also shown Figs. 11 and 12. Noting that in several cases (with very thick plates, normally t/b or t/h are greater than 0.1) the plates have very important plastic deformation and the buckling loads are not visible. In these cases, the plastic loads with the elastic-perfectly plastic material assumption are used instead of the buckling load concept. The values of μ_1 given in Table 3 are only used for the outside plate with rectangular form. With the case of triangular form of the outside plate, for the sake of simplification in the

practices, $0,9\mu_1$ can be approximated, this value is observed from the numerical analysis results. In the calculation of μ_1 and μ_2 given in Tables 3 and 4, the buckling stresses ($\sigma_{\text{numerical}}$ in Eqs.(7) and (8)) are defined as the following:

$$\sigma_{\text{buckling}} = \frac{p}{2t} \text{ for the outside part,} \quad (9)$$

$$\sigma_{\text{buckling}} = \frac{\max(|q_s|, |q_i|)}{t} \text{ for the inside part.} \quad (10)$$

p , q_s and q_i in Eqs.(9) and (10) are the values at the critical states of the plates in the FE analysis, the relation of these quantities with the applied loads, V_{Ed} and F_{Ed} , are described by Eqs.(1), (2) and (3).

4. Model validation for the inside part of the through-plate

This section presents the validation of the proposed model for the through-plate by using the experimental results. The main objective is the validation of the assumptions (1) and (2) (as mentioned in Section 2) and the FE model presented in Section 3. Therefore, the proposed models of the plate (Fig.4), the actual material and geometries of the through-plates are introduced in the FE analysis for obtaining the critical loads that are used to compare with experimental data.

4.1. Experimental tests

Three tests on the inside part of the through-plate were performed at Thessaly University within ATTEL project, the test set-up is outlined on Fig. 13, and the detail on the tests can be found in [10]. As the aim is oriented to study the inside part of the through-plate component, the concrete slab is replaced by a rigid link that almost supports only the tension force. Also, as the bolts are not the objectives then the steel beams are directly welded to the through plate. The main geometries of the three specimens are reported on Table 5. The mean values of the yield strength and the ultimate strength of the through plates given by coupon tests are 418 N/mm² and 602 N/mm², respectively. Among the results given by the tests, the maximal bending moments (M_{max} on Fig.13) and the failure modes (Fig.14) are used to validate the proposed formulas.

4.2. Calculation of the resistance of the tested through- plate

As the maximal bending moment (M_{\max}) is used to compare, the applied loads on the through-plate need to be written under the function of M_{\max} .

- The vertical load (V_{Ed}) equals to the reaction of the supports (Fig.13):

$$V_{Ed} = M_{\max} / l_1. \quad (11)$$

- As the bending moment at the middle point of the weld lines between the through-plate and the beam flange (point A on Fig.13) is used to calculate the horizontal load, F_{Ed} , this force can be written under the function of the maximal moment by:

$$F_{Ed} = M_A / d = M_{\max} (l_2 / l_1) / d. \quad (12)$$

Substituting V_{Ed} and F_{Ed} in Eqs.(11) and (12) into Eqs.(3) and (4) one obtains $q_i = 0.625q_s$ for specimens 1 and 2; and $q_i = 0.183q_s$ for specimen 3. These load distributions are introduced in the FE model with the boundary conditions and initial imperfection shown on Figs.4 and 9, respectively. Concerning the material modelling, the actual curve with the measured values of the yield strength and the ultimate strength are used.

4.3. Comparison and discussions

The calculated and tested values of the maximal bending moments are compared, as summarized in Table 6 and on Fig.15. The comparisons on the complete curves are not dealt with because the experimental curves including the deformation of the test set-up system (steel beam, set-up joints, etc.) that did not introduce in the calculated curves. From the comparison with the experimental results, it can be said that the accuracy of the proposed model on the resistance of the through-plate can respond to the practical purpose.

As the examples, the resistance of the tested specimens will be also calculated by using the proposed design procedure in Section 5.

5. Design procedure

The design procedure for verifying the resistance of the through-plate components can be now summarized as follows.

Step 1: determining the applied loads on the connection, V_{Ed} and F_{Ed} . V_{Ed} equals to the design value of the shear force at the beam end while F_{Ed} equals to the ratio of the design bending moment at the connection to the height of the joint, the last is the distance between the gravity centre of the rebars to the upper side of the through plate.

Step 2: calculating the load direction for the outside part, $\alpha = \arctan \frac{V_{Ed}}{F_{Ed}}$; and the load parameters, q_s and q_i , for the inside part by using Eqs.(3) and (4).

Step 3: with the load and dimension parameters, computing the coefficients μ_1 and μ_2 from Tables 3 and 4 in which the linear interpolation can be applied for the intermediate points.

Step 4: verifying the resistance of the through-plate by using the following expressions, Eqs.(13) and (14):

$$\frac{V_{Ed}}{t(b-c)} \leq \kappa \mu_1 \frac{\pi^2 E}{12(1-\nu^2)} \left(\frac{t}{b} \right)^2 / \gamma_M \text{ for the outside part} \quad (13)$$

$$\max \left(\left| \frac{4F_{Ed}}{th} - \frac{V_{Ed}(4b+2c)}{th^2} \right|, \left| \frac{V_{Ed}(4b+2c)}{th^2} - \frac{2F_{Ed}}{th} \right| \right) \leq \mu_2 \frac{\pi^2 E}{12(1-\nu^2)} \left(\frac{t}{h} \right)^2 / \gamma_M \text{ for the inside part} \quad (14)$$

with γ_M is the partial factor, the value of 1.25 is recommended for this case; κ is a coefficient taking into account the shape of the outside plate, $\kappa = 1.0$ for the rectangular form and $\kappa = 0.9$ for the triangular form; μ_1 and μ_2 are given in Tables 3 and 4. Noting that Eqs. (13) and (14) are deduced from Eqs.(1), (3), (4), (7), (8), (9) and (10).

Numerical example: the resistance of three tested specimens, through the maximal bending moment (M_{max}), are calculated by the above procedure and the main results are presented in Table 7. In comparison with the maximal moments given by the tests (Table 6), the calculated moments (Table 7) are conservatives, the explanations are that: (1) the actual strength of the material, 418 N/mm², are greater than 355 N/mm² – the introduced value in the models; (2) the partial factor $\gamma_M=1,25$ is used.

Remarks: the above development is devoted to two-side joints, in the case of one-side joints (i.e. in the external columns) the proposed joint configuration, but without one outside part, can be used. The formulas concerning the outside part are still suitable for this case while a quite large conservative is observed for using the formulas related to the inside part. However, in order to avoid the important transverse shear in the column and also the local bending in the column wall, the hinge model is recommended for the one-side joints in the proposed building frame-type; the slab reinforcement detail should be accordingly adopted.

6. Conclusions

A configuration for beam-to-column joint with steel hollow section column is proposed in this paper. This type of beam-to-column joint is recommended for using in buildings subjected to static loading with the vertical load being preponderant in comparison with horizontal load. The economic benefit of using high strength steel tubes for the columns is identified in this kind of buildings [2]. The main component of the joint is a through-plate passing through the column and supporting the steel beams. The calculation procedure for the resistance of the through-plate component is developed. The development is based on the linear elastic buckling theory of thin plates while the plasticity of the material, the geometrical imperfection, and the shear effect of thick plates are taken into account by numerical way. The design procedure for the investigated component is proposed, from which in knowing the applied loads, the geometries and the materials, the resistance of the component can be directly determined. The results given by the proposed design model are validated by experimental data showing that the accuracy responds to the practical purpose.

Acknowledgements

This work was carried out with a financial grant from the Research Fund for Coal and Steel of the European Community, within ATTEL project: “Performance-Based Approaches for High Strength Steel Tubular Columns and Connections under Earthquake and Fire Loadings”, Grant N^o RFSR-CT-2008-00037.

References

- [1] ATTEL project: “Performance-based approaches for high-strength tubular columns and connections under earthquake and fire loadings”, Final Report, 2012, <http://orbi.ulg.ac.be/handle/2268/126526>
- [2] Hoang V.L., Demonceau J.F, Ly D.P.L, Rossi B. Field of application of high strength steel circular tubes for steel and composite columns from an economic point of view. *Journal of Constructional Steel Research*, 2011 (67):1001-1021.
- [3] Hoang V.L., Demonceau J.F., Jaspart J.P. Proposal of a simplified analytical approach for the characterisation of the end-plate component in circular tube connection. *Journal of Constructional Steel Research*, 2013 (90): 245-252.
- [4] Anderson D (ed). COST C1 - Composite steel-concrete joints in frames for buildings: Design provisions. Brussels – Luxembourg 1999.
- [5] Eurocode 3: Design of steel structures - Part 1-8: Design of joints. EN 1993-1-8, Brussels, 2003.
- [6] LAGAMINE: User’s manual, University of Liege, 2010.
- [7] Blicch F. Buckling Strength of metal structures. McGraw-Hill, New York, 1952.
- [8] Wang C.M., Xiang Y., Chacrabarty J. Elastic/plastic buckling of thick plates. *International journal of Solids and Structures*, 2001 (38): 8617-8640.
- [9] Eurocode 3: Design of steel structures - Part 1-5: Plated structural elements. EN 1993-1-5, Brussels, 2003.
- [10] ATTEL project: “Performance-based approaches for high-strength tubular columns and connections under earthquake and fire loadings”, Deliverable Report D.3: simulation data relevant to the selected typologies of base joints, of HSS-CHS columns and HSS-CFT column and of HSS-concrete composite beam-to-column joints, 2012, <http://orbi.ulg.ac.be/handle/2268/126857>

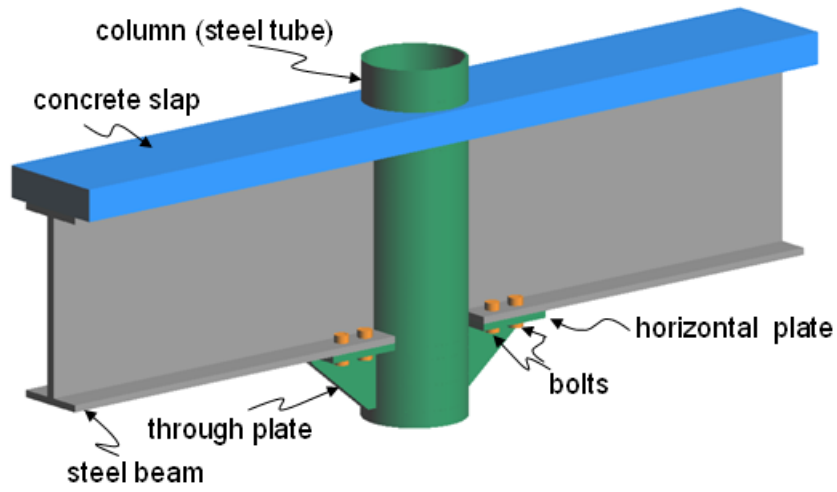


Fig.1. Proposed beam-to-column joint configuration

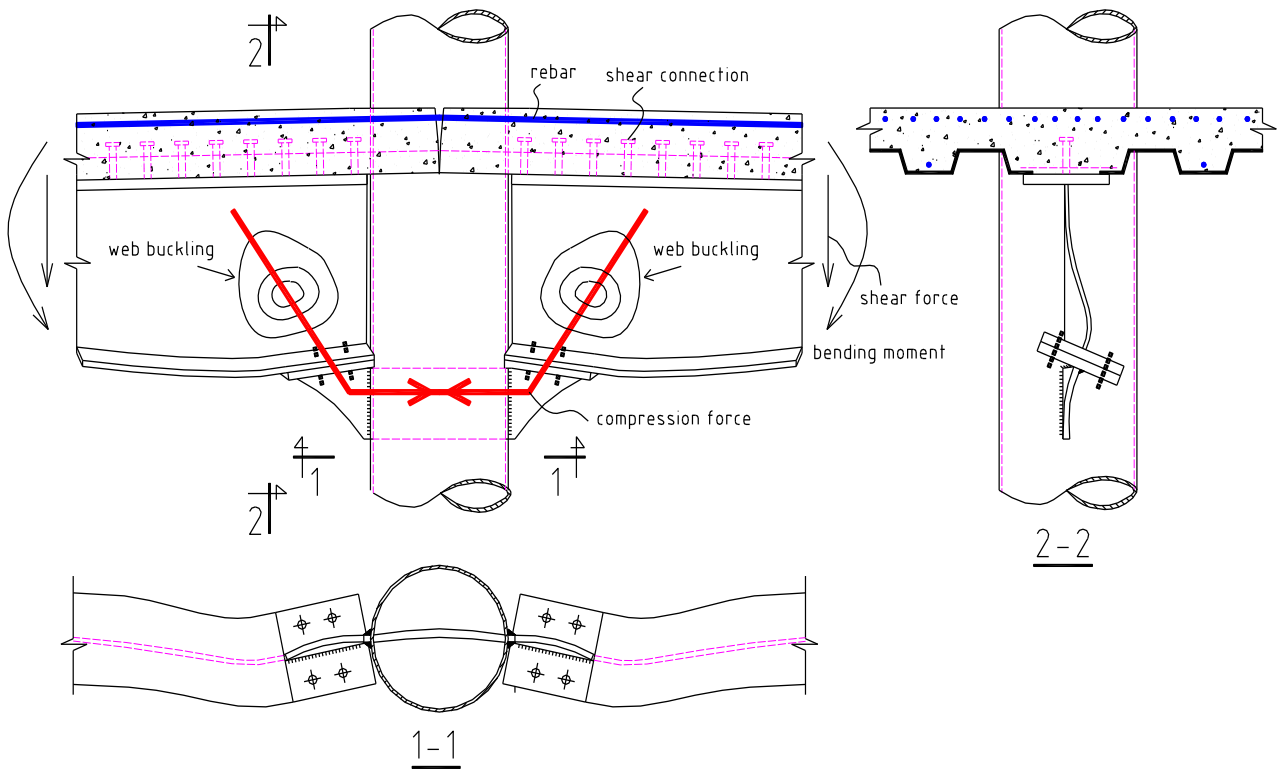


Fig.2. Considered buckling mode for the joint

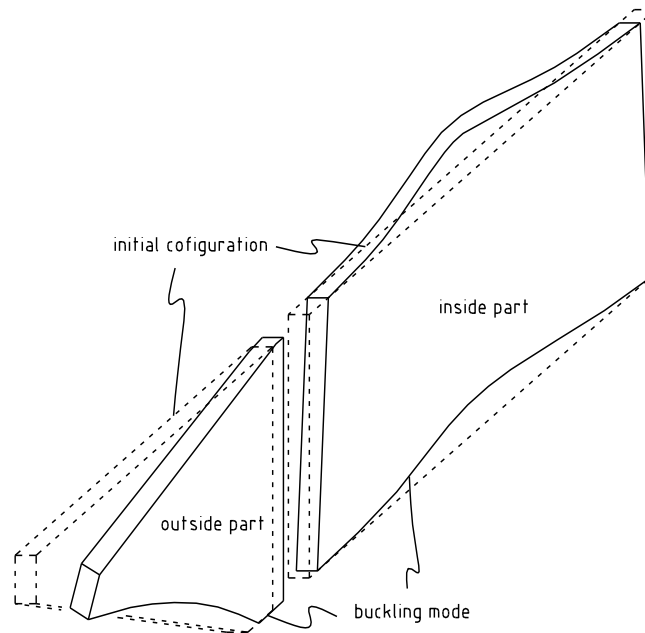


Fig.3. Buckling mode of the through plate

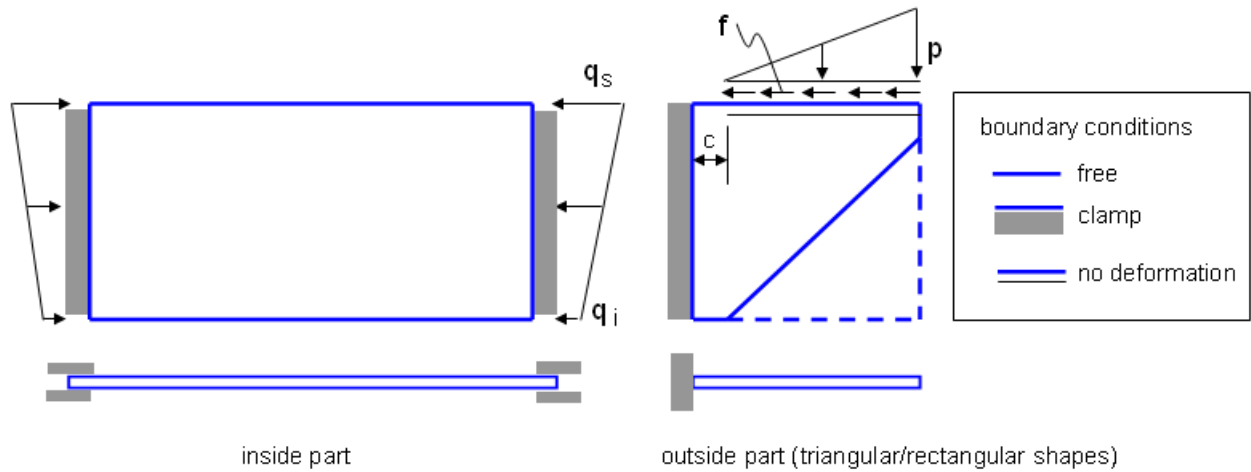


Fig.4. Boundary and loading modellings for the through-plate

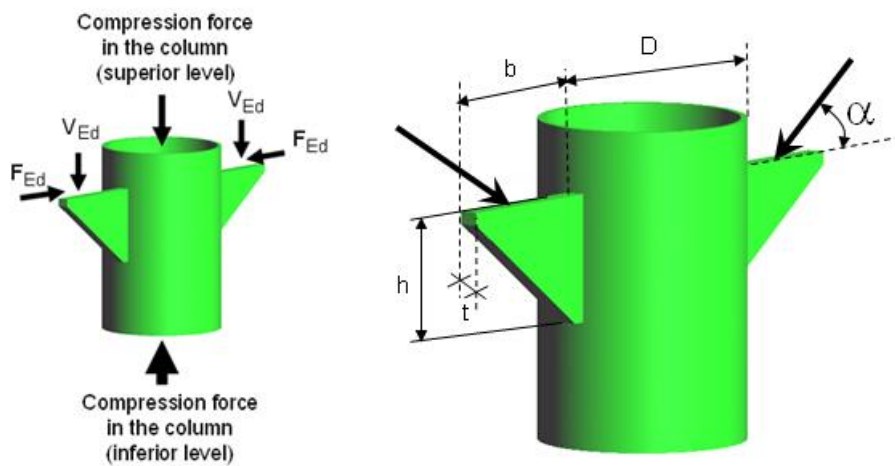


Fig.5. Notations on the through-plate component

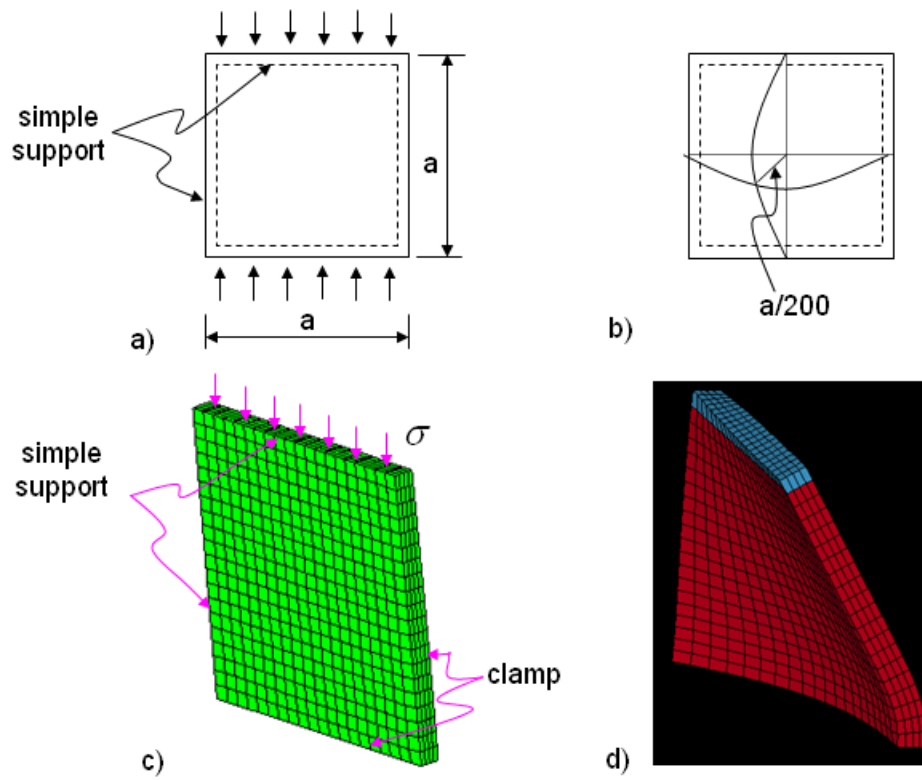


Fig.6. Example 1: a) plate description b) initial imperfection used in LAGAMINE; c) FE modelling in LAGAMINE (1/4 part); d) Buckling mode given by LAGAMINE

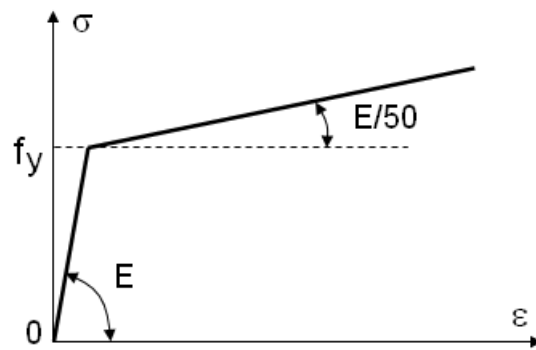


Fig.7. Material modelling in the numerical analysis

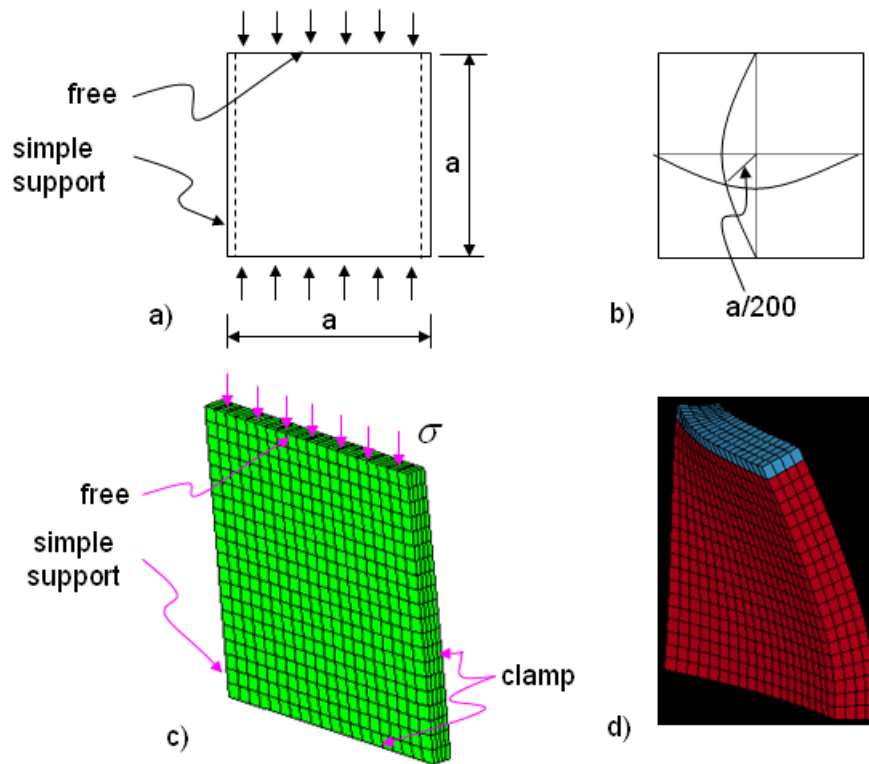


Fig.8. Example 2: a) plate description b) initial imperfection used in LAGAMINE; c) FE modelling in LAGAMINE; d) Buckling mode given by LAGAMINE

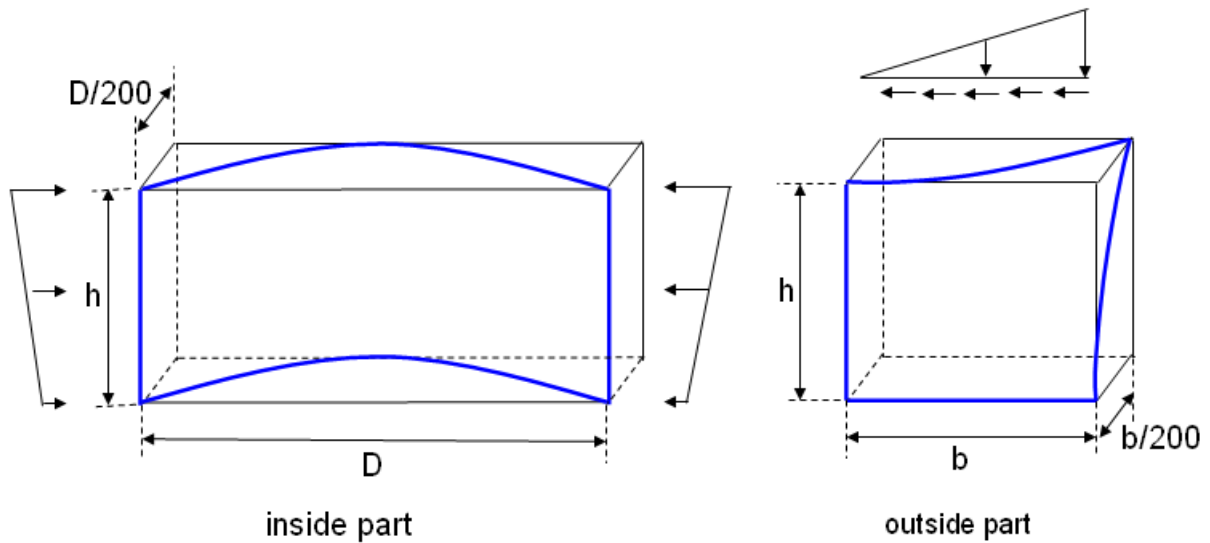


Fig.9. Modelling of the geometric imperfection for the plates

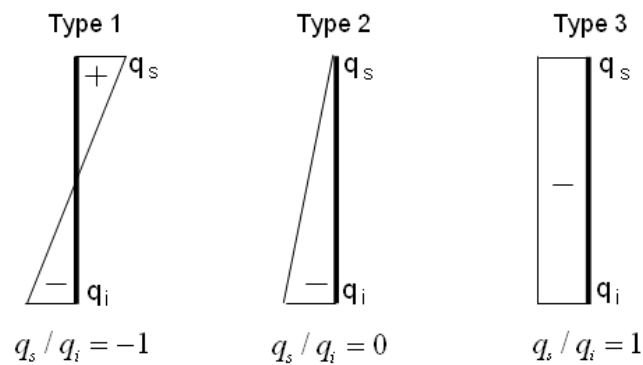


Fig.10. Loading types for the inside plate

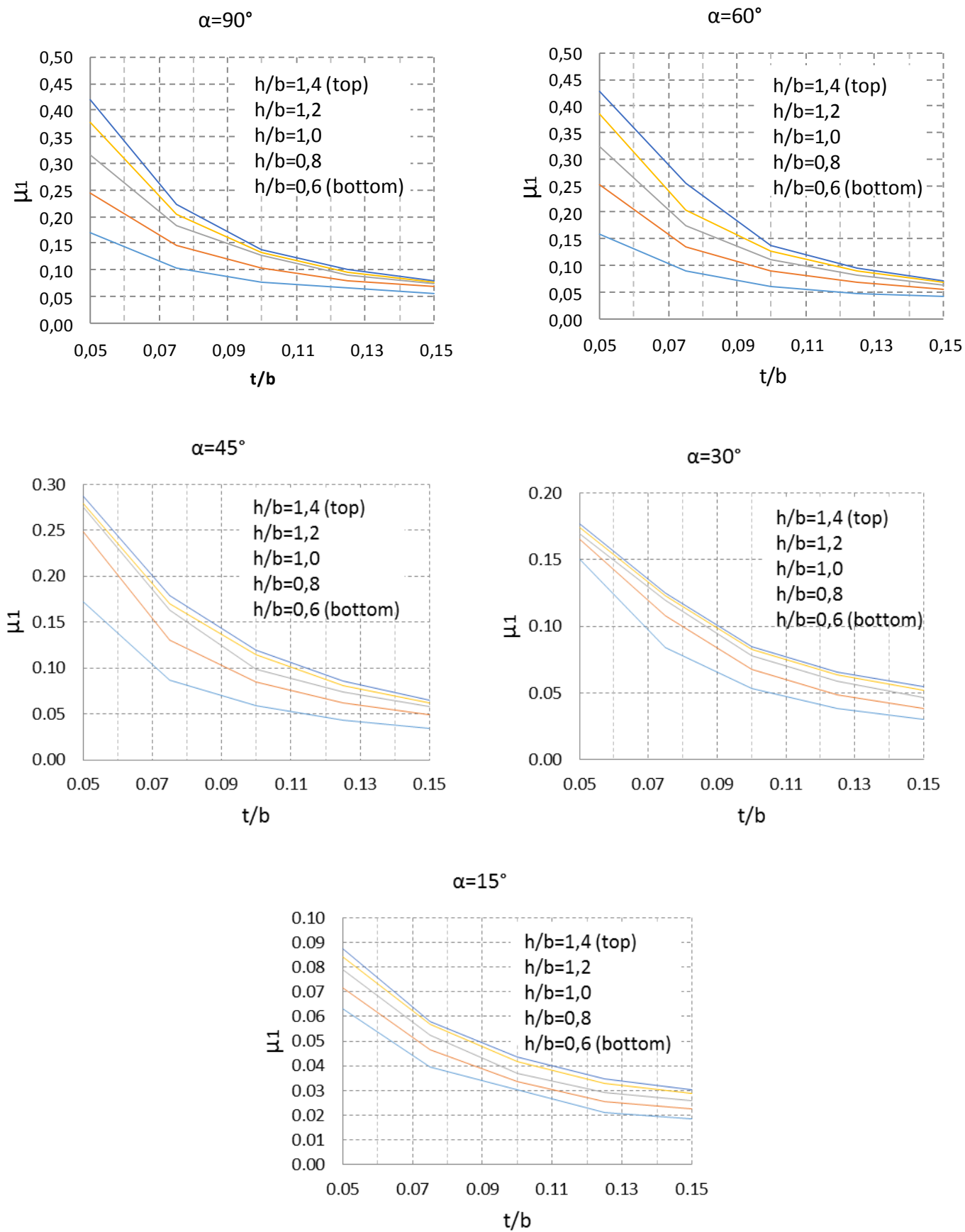


Fig.11. Coefficient μ_1

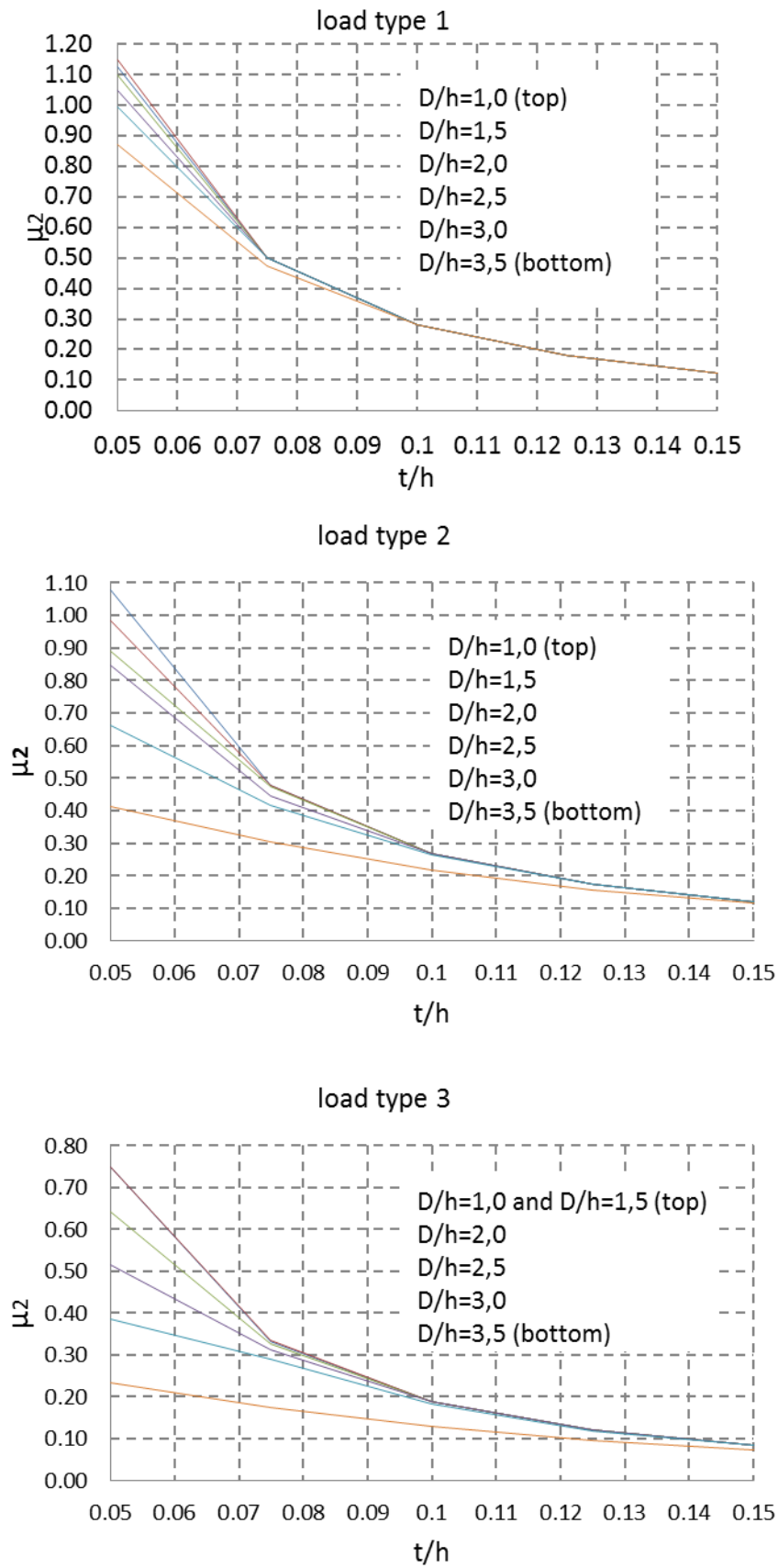


Fig.12. Coefficient μ_2



Fig.14. Buckling mode of the tested through-plates (inside part)

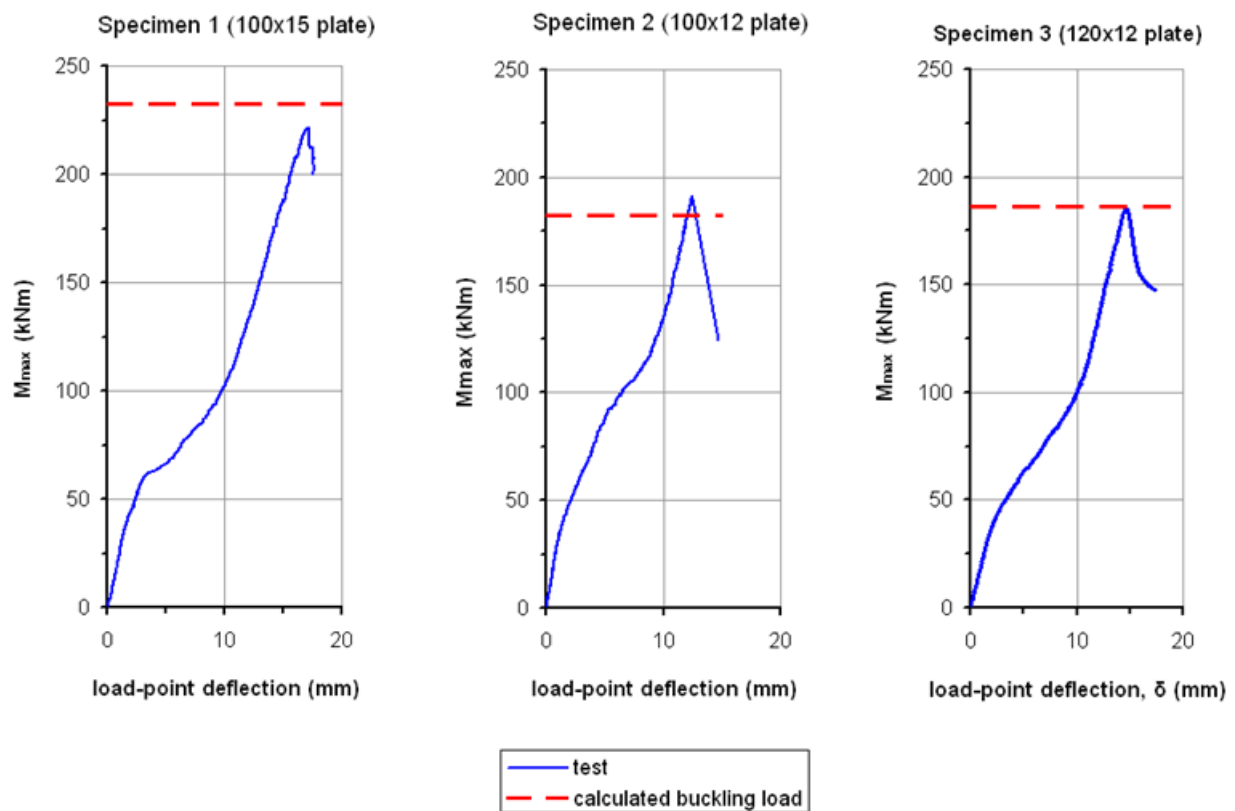


Fig.15. Test and modelling comparison on the buckling load

Table 1: example 1 - comparison of results

b/t	Buckling stress (in ksi)			
	IT [8]	DT [8]	Bliech's theory ^(*)	LAGAMINE
22	70.844	60.080	56.125	51.460
23	65.166	58.836	55.139	50.366
24	60.713	57.397	54.109	49.258
25	57.363	55.730	52.988	48.090
26	54.598	53.806	51.712	47.289
27	51.938	51.569	50.185	46.520
28	49.112	48.962	48.269	45.642

Remark: (*) these values are calculated by Wang et al [8] from the formulas given by Bliech [7].

Table 2: example 2- comparison of results

E/σ_0	Buckling stress factor $\sigma_c \frac{12(1-\nu^2)}{\pi^2 E} \left(\frac{a}{t}\right)^2$		
	IT [8]	DT [8]	LAGAMINE
200	1.136	0.999	0.966
300	1.104	0.819	0.686
500	1.104	0.473	0.434
750	1.104	0.298	0.215

Table 3: Buckling stress factor for outside plate (μ_1)

Geometries		Load direction (in degree)				
h/b	t/b	$\alpha=90$	$\alpha=60$	$\alpha=45$	$\alpha=30$	$\alpha=15$
0,60	0,050	0,1686	0,1591	0,1718	0,1500	0,0632
	0,075	0,1027	0,0887	0,0871	0,0840	0,0397
	0,100	0,0763	0,0610	0,0589	0,0531	0,0302
	0,125	0,0661	0,0475	0,0433	0,0381	0,0213
	0,150	0,0546	0,0402	0,0343	0,0304	0,0185
0,80	0,050	0,2455	0,2518	0,2487	0,1654	0,0717
	0,075	0,1467	0,1343	0,1308	0,1080	0,0465
	0,100	0,1027	0,0902	0,0844	0,0677	0,0337
	0,125	0,0801	0,0672	0,0620	0,0488	0,0255
	0,150	0,0699	0,0543	0,0492	0,0384	0,0225
1,00	0,050	0,3151	0,3246	0,2750	0,1695	0,0790
	0,075	0,1820	0,1758	0,1636	0,1195	0,0525
	0,100	0,1263	0,1117	0,0985	0,0778	0,0370
	0,125	0,0908	0,0812	0,0742	0,0591	0,0293
	0,150	0,0744	0,0640	0,0582	0,0464	0,0260
1,20	0,050	0,3762	0,3857	0,2792	0,1739	0,0843
	0,075	0,2042	0,2039	0,1700	0,1230	0,0568
	0,100	0,1317	0,1263	0,1142	0,0829	0,0419
	0,125	0,0961	0,0893	0,0807	0,0637	0,0331
	0,150	0,0765	0,0691	0,0624	0,0520	0,0288
1,40	0,050	0,4194	0,4278	0,2870	0,1770	0,0875
	0,075	0,2217	0,2535	0,1789	0,1250	0,0580
	0,100	0,1386	0,1374	0,1191	0,0844	0,0436
	0,125	0,0993	0,0943	0,0859	0,0658	0,0348
	0,150	0,0786	0,0713	0,0654	0,0546	0,0304

Table 4: Buckling stress factor for inside plate

Geometries		Load type (Fig.10)		
D/h	t/h	type 1	type 2	type 3
1,00	0,050	1,1233	1,0790	0,7482
	0,075	0,4989	0,4796	0,3310
	0,100	0,2806	0,2698	0,1870
	0,125	0,1795	0,1725	0,1194
	0,150	0,1247	0,1198	0,0831
1,50	0,050	1,1465	0,9842	0,7482
	0,075	0,4989	0,4796	0,3335
	0,100	0,2806	0,2698	0,1870
	0,125	0,1795	0,1725	0,1194
	0,150	0,1247	0,1198	0,0831
2,00	0,050	1,0959	0,8915	0,6407
	0,075	0,4989	0,4758	0,3253
	0,100	0,2806	0,2698	0,1873
	0,125	0,1795	0,1725	0,1194
	0,150	0,1247	0,1198	0,0831
2,50	0,050	1,0453	0,8472	0,5142
	0,075	0,4989	0,4452	0,3122
	0,100	0,2806	0,2698	0,1873
	0,125	0,1795	0,1725	0,1194
	0,150	0,1247	0,1198	0,0831
3,00	0,050	0,9926	0,6617	0,3857
	0,075	0,4989	0,4146	0,2897
	0,100	0,2806	0,2634	0,1839
	0,125	0,1795	0,1725	0,1188
	0,150	0,1247	0,1198	0,0830
3,50	0,050	0,8690	0,4135	0,2321
	0,075	0,4750	0,3043	0,1755
	0,100	0,2806	0,2170	0,1292
	0,125	0,1795	0,1558	0,0959
	0,150	0,1247	0,1150	0,0715

Table 5: geometries of the tested specimens

Specimen	Height of through plate, h (mm)	Thickness of through plate, t (mm)
1	100	15
2	100	12
3	120	12
For the all specimens: 324x10 tube is used; c = 20mm; d = 327.5 mm (Fig.13).		

Table 6: Comparison on the maximal bending moment and failure modes

Specimen	Maximal bending moment (kNm)	
	Tested values [2]	Calculated values
1 (100x15 plate)	221.2	232.5
2 (100x12 plate)	191.2	182.2
3 (120x12 plate)	185.4	186.3
The same buckling modes are identified in both numerical analysis and experimental tests.		

Table 7: numerical examples for design procedure

Step	Quantities (*)	Specimen 1	Specimen 2	Specimen 3	Reference
1	t/h	0,15	0,12	0,1	See Table 5
	D/h	3,24	3,24	2,7	
	V _{Ed}	M _{max} /1,578	M _{max} /1,578	M _{max} /1,578	Eq.(11)
	F _{Ed}	M _{max} /0,405	M _{max} /0,405	M _{max} /0,405	Eq.(12)
2	q _s	30,32 M _{max}	30,32 M _{max}	34,77 M _{max}	Eq.(3)
	q _i	19,06 M _{max}	19,06 M _{max}	6,38 M _{max}	Eq.(4)
	q _i /q _s	0,63	0,63	0,18	
3	μ ₂	0,0923	0,1407	0,2259	Table A2 (*)
4	M _{Rd}	155,80	121,63	132,12	Eq.(14)

Remarks: (*) units in kN and m

(**) linear interpolations are applied